

CLASSIFICATION OF SOIL STIFFNESS USING P-WAVE

ROSE NADIA BINTI ABU SAMAH

UNIVERSITI SAINS MALAYSIA

2016

CLASSIFICATION OF SOIL STIFFNESS USING P-WAVE

by

ROSE NADIA BINTI ABU SAMAH

**Thesis submitted in fulfillment of the
requirements for the degree of
Master of Science**

August 2016

ACKNOWLEDGMENT

Alhamdulillah. Thanks to Allah SWT for His mercy and guidance in giving me opportunities and strength to complete this thesis. I would like to express my sincere appreciation to my supervisor, Associate Professor Dr. Rosli Saad for his continuous encouragement, guidance and cooperation. I would also like to express my grateful thanks to Dr. Nordiana Binti Mohd Muztaza, Dr. Nur Azwin Binti Ismail and Dr. Andy Anderson Anak Bery for their uncountable support and suggestions throughout the preparation of this thesis.

Special thanks and appreciation to geophysics technical staff for their great commitment and assistance – Mr. Yaakub Bin Othman, Mr. Azmi Bin Abdullah and Mr. Abdul Jamil Bin Yusuff. Deepest gratitude to my awesome postgraduate friends, Mr. Tarmizi, Mr. Fauzi Andika, Mr. Muhammad Taqiuddin Bin Zakaria, Mr. Kiu Yap Chong, Mr. Hazrul Hisham Bin Badrul Hisham, Mr. Muhammad Afiq Bin Saharudin, Mr. Yakubu Mingyi, Mr. Muhammad Sabiu Bala, Mr. Sabrian Tri Anda, Mr. Amsir, Ms. Umi Maslinda Binti Anuar, Ms. Nur Amalina Binti Mohd Khoirul Anuar and Ms. Nordiana Binti Ahmad Nawawi.

Last but not least, million thanks to my parents, Wan Awang Bin Wan Abdul Rahman and Zawani Binti Abd. Ghani for their prayers, love, care, encouragement, understanding and support throughout the completion of this thesis, from beginning till the end.

TABLE OF CONTENTS

Acknowledgment	ii
Table of contents	iii
List of tables	vi
List of figures	vii
List of symbols	ix
List of abbreviations	x
Abstrak	xi
Abstract	xii
CHAPTER 1: INTRODUCTION	1
1.0 Preface	1
1.1 Problem statement	2
1.2 Objective of study	2
1.3 Scope of study	2
1.4 Thesis layout	3
CHAPTER 2: LITERATURE REVIEW	4
2.0 Introduction	4
2.1 Theory background	4
2.1.1 Elastic wave	5

2.1.2	Wave's propagation principle	8
2.1.3	Homogeneous subsurface	10
2.1.4	Single subsurface interface (2 Layer case)	12
2.1.5	Factors effecting velocity	14
2.2	Geotechnical investigation	15
2.2.1	Rotary wash boring (RWB)	16
2.2.2	Standard Penetration Test (SPT)	16
2.3	Previous study	17
2.4	Chapter summary	26
CHAPTER 3: MATERIALS AND METHODS		28
3.0	Introduction	28
3.1	Study flow	29
3.1.1	Preliminary study	29
3.1.2	Seismic refraction tomography (SRT)	30
3.1.3	Drilling method	31
3.1.4	Data processing	32
3.1.5	Data analysis	33
3.2	Study area	34
3.2.1	General geology and geomorphology of USM	34
3.2.2	General geology and geomorphology of Sungai Batu	37
3.2.3	Survey line	39
3.3	Chapter summary	41

CHAPTER 4: RESULTS AND DISCUSSION	42
4.0 Preface	42
4.1 Geophysical results and discussion	42
4.1.1 USM, Pulau Pinang	42
4.1.2 Sungai Batu	43
4.2 Geotechnical results	46
4.2.1 USM, Pulau Pinang	46
4.2.2 Sungai Batu	47
4.3 Geophysical and geotechnical correlation	47
4.3.1 USM, Pulau Pinang	48
4.3.2 Sungai Batu	54
4.4 Chapter summary	62
CHAPTER 5: CONCLUSION AND RECOMMENDATIONS	63
5.1 Recommendations	64
REFERENCES	65
APPENDIXES	
LIST OF PUBLICATIONS	

LIST OF TABLES

		Page
Table 2.1	P-wave velocity of common materials	15
Table 2.2	Impacted soil and rock standard table for inside crater of Bukit Bunuh impact crater	18
Table 2.3	Impacted soil and rock standard table on rim/slumped terrace of Bukit Bunuh impact crater	18
Table 2.4	Impacted soil and rock standard table for outside crater of Bukit Bunuh impact crater	19
Table 2.5	Velocity comparison with previous study	19
Table 2.6	The relation between V_p , V_s , N-value and density	20
Table 3.1	List of equipment for seismic refraction survey	30
Table 3.2	Categories of absolute correlation strength, R	34
Table 3.3	Survey line and borehole in USM and Sungai Batu	41
Table 4.1	Location and depth of borehole at USM, Pulau Pinang	46
Table 4.2	Location and depth of borehole at Sungai Batu, Kedah	47
Table 4.3	Correlation between N-value and P-wave velocity of granite residual soil at USM, Pulau Pinang	52
Table 4.4	Soil strength classifications of P-wave velocity (V_p) and N-value of granite residual soil at USM, Pulau Pinang	53
Table 4.5	Comparison of research result with previous study	54
Table 4.6	Correlation between N-value and P-wave velocity of alluvium at Sungai Batu	61
Table 4.7	P-wave velocity and N-value classification of Sungai Batu alluvium	61

LIST OF FIGURES

	Page	
Figure 2.1	Particle move parallel to the direction of wave propagation	5
Figure 2.2	Particle move perpendicular to the direction of S-waves propagation	6
Figure 2.3	Rayleigh wave; particle experience elliptical retrograde motion due to the combination of compressional and vertical shear (SV) waves	7
Figure 2.4	Ground particle move side-to-side, perpendicular to the Love wave's propagation	8
Figure 2.5	Wavefront position at t_2 after an interval of time Δt using Huygens' Principle	9
Figure 2.6	Schematic diagram of Snell's Law	10
Figure 2.7	Ray paths in homogeneous subsurface	11
Figure 2.8	Refracted ray path for a single subsurface interface	12
Figure 2.9	Travel time curve for a single subsurface interface	12
Figure 2.10	Standard penetration test method	17
Figure 2.11	Empirical correlation of (a) P-wave velocities with N-values and (b) P-wave velocities with RQD values for both studied areas	21
Figure 3.1	Research methodology flow chart	29
Figure 3.2	Seismic equipment's setting	30
Figure 3.3	Equipment for seismic refraction tomography survey	31
Figure 3.4	Rotary wash boring rig	32
Figure 3.5	Seismic data processing flowchart	33
Figure 3.6	Location of survey area, USM, Pulau Pinang	35
Figure 3.7	Location of Pulau Pinang	36

Figure 3.8	General geology of Pulau Pinang	37
Figure 3.9	Location of Sungai Batu, Kedah	38
Figure 3.10	Geology map of Sungai Batu, Kedah (Geological Map of Peninsular Malaysia)	39
Figure 3.11	USM survey line	40
Figure 3.12	Five survey lines at Sungai Batu, Kedah	40
Figure 4.1	Seismic velocity distribution along survey line, L1 at USM, Pulau Pinang	43
Figure 4.2	Seismic velocity distribution of line L2 at Sungai Batu, Kedah.	44
Figure 4.3	Seismic velocity distribution at Sungai Batu, Kedah; a) L3 and b) L4	45
Figure 4.4	Seismic velocity distribution at Sungai Batu, Kedah; a) L5 and b) L6	45
Figure 4.5	Correlation of seismic velocity section with boreholes record at USM, Pulau Pinang	49
Figure 4.6	Relation between V_p and N-value against depth for BH1 and BH2, USM	50
Figure 4.7	Graph of N-value against P-wave velocity for BH1, USM	51
Figure 4.8	Graph of N-value against P-wave velocity for BH2, USM	51
Figure 4.9	Correlation of seismic velocity section of line L3 with boreholes BH3 at Sungai Batu	55
Figure 4.10	Correlation of seismic velocity section of line L4 with borehole BH4 at Sungai Batu	56
Figure 4.11	Correlation of seismic velocity section of line L5 with borehole BH5 at Sungai Batu	57
Figure 4.12	Correlation of seismic velocity section of line L6 with borehole BH6 at Sungai Batu	58
Figure 4.13	Relation between V_p and N-value against borehole depth at Sungai Batu; (a) BH3, (b) BH4, (c) BH5 and (d) BH6	59
Figure 4.14	Graphs of N-value against P-wave velocity for borehole at Sungai Batu; (a) BH3, (b) BH4, (c) BH5 and (d) BH6	60

LIST OF SYMBOLS

$\frac{dt}{dx}$	First derivative with respect to x
h_1	Thickness of first layer
K	Bulk modulus
m	Meter
m/s	Meter per second
t	Time travel
Δt	Time interval
x	Distance
ρ	Density
μ	Shear modulus
π	Pi
θ_i	Incidence angle
θ_r	Refracted angle
θ_{ic}	Critical angle of incidence
<	Less than
>	Greater than
°	Degree
'	Minutes
"	Second

LIST OF ABBREVIATIONS

3-D	Three dimension
BH	Borehole
HWAW	Harmonic wavelet analysis of waves
IT	Intercept-time
LL	Liquid limit
MASW	Multichannel analysis of surface wave
MC	Moisture content
PI	Plastic index
PL	Plastic limit
R ²	Regression
RWB	Rotary wash boring
SASW	Spectral analysis of surface wave
SCPT	Seismic cone penetration test
SPT	Standard penetration test
SRT	Seismic refraction tomography
USM	Universiti Sains Malaysia

PENGKELASAN KETEKALAN TANAH MENGGUNAKAN GELOMBANG-P

ABSTRAK

Tomografi seismik biasan (SRT) adalah satu kaedah geofizik yang mengukur perambatan gelombang bunyi di bawah permukaan bumi. Kaedah ini memerlukan tenaga tiruan sebagai sumber. Antara sumber-sumber tenaga adalah tukul eretan, jatuhan pemberat dan dinamit. Objektif kajian adalah penting untuk menentukan jenis sumber tenaga yang paling sesuai. Dalam kajian ini, objektif adalah untuk menentukan halaju gelombang-P bagi tanah baki granit dan sedimen, akhir sekali, mengenal pasti hubungan antara halaju gelombang-P dan nilai-N bagi sub-permukaan tersebut. Data diproses menggunakan perisian FirstPix, SeisOpt@2D dan surfer8. Kajian ini dijalankan di Universiti Sains Malaysia (USM), Minden dan Sungai Batu, Kedah. Geologi kedua-dua kawasan dilapisi oleh formasi Mahang yang terdiri daripada urutan syal gelap dan chert diselangi batu pasir. Halaju gelombang-P bagi tanah baki granit dan sedimen berjaya ditentukan. USM mempunyai 3 lapisan halaju sub-permukaan iaitu; 400-700 m/s dengan nilai-N adalah 3-17, 700-2800 m/s dengan nilai-N adalah 9-45 dan >2976 m/s dengan nilai-N >50 yang merujuk kepada lapisan yang pertama, kedua dan ketiga. Sub-permukaan tapak Sungai Batu juga terdiri daripada 3 lapisan halaju; <1500 m/s dengan nilai-N adalah 7-32 merupakan lapisan yang pertama, 1500-5000 m/s dengan nilai-N adalah 11-50 merupakan lapisan kedua dan >5000 m/s dengan nilai-N >50 adalah batuan dasar. Kajian menunjukkan kaedah tomografi seismik biasan adalah sesuai digunakan bagi kajian ketekalan tanah baki granit dan sedimen.

CLASSIFICATION OF SOIL STIFFNESS USING P-WAVE

ABSTRACT

Seismic refraction tomography (SRT) is a geophysical method that measures the propagation of sound wave in Earth's subsurface. This method required an artificial energy as a seismic source. Several types of energy sources are sledge hammer, weight drop and dynamite. Objective of a survey is crucial in determining the most suitable type of energy source. In this research, the objectives are to determine subsurface P-waves velocity of granite residual soil and sediment, finally, to identify relationship between the P-waves velocity and N-value of the subsurface. The data were processed using FirstPix, SeisOpt@2D and surfer8. This research was conducted in Universiti Sains Malaysia (USM), Minden and Sungai Batu, Kedah. Geologically, both areas were underlain by Mahang formation which describes as a sequence of dark shale and chert with interbeds of sandstone. P-wave velocity of the residual soil and sediment were successfully determined. USM consists of 3 subsurface velocity layer which are; 400-700 m/s with N-value of 3-17, 700-2800 m/s with N-value of 9-45 and >2976 m/s with N-value of >50 which are first, second and third layer respectively. Sungai Batu site also indicates a 3 subsurface velocity layers; <1500 m/s with N-value of 7-32 being the first layer, 1500-5000 m/s with N-value of 11-50 as the second layer and >5000 m/s with N-value of >50 is the bedrock. Studies shows that seismic refraction tomography method is suitable for stiffness investigation of granite residual soil and sediment.

CHAPTER 1

INTRODUCTION

1.0 Preface

Seismic refraction is one of non-intrusive geophysical method using primary wave (P-wave) or compressional wave to measure the wave velocity propagating through subsurface profile. The velocity profile carries information on the type of sediment or rock. This technique is crucial not only for structural information, such as delineating valley or faults structures, but is also often used as physical characterization of layers and thus is very useful in geotechnical investigations. The seismic wave velocity depends upon elasticity and density of the soil and rock through which it propagate (Burger, 1992).

In this multidisciplinary era, geophysical methods are widely utilized in engineering investigations such as subsurface characterization (depth to bedrock, rock type, water table and locating fractures), highway subsidence (detecting cavities and sinkholes) and engineering properties of Earth material (stiffness, density and porosity) (Soupis et al., 2007; Anderson and Croxton, 2008; Abidin et al., 2011; Ismail et al., 2013). Realizing the role of geophysics in engineering fields, many studies are conducted to comprehend the relationship between geophysical methods and geotechnical ground properties to ensure reliable interpretation. The understanding of geophysical and geotechnical correlation increase the effectiveness of civil engineering works and also reduce the survey cost.

1.1 Problem statement

Drilling method is popular and widely utilized in geotechnical investigations. However, the data generated is limited to a particular point. Hence, to cover a large site require a number of boreholes which results to higher cost and longer time of investigation. To overcome these problems, researcher attempts to correlate N-value with shear wave (S-wave) velocity, primary wave (P-wave) velocity, rock quality designation (RQD) and other geotechnical properties to produce an empirical correlation between the parameters. However, this research is attempted to produce a standard correlation table between P-wave velocity and N-value for residual soil and sedimentary study area. This correlation can be a guide in estimating the N-value from P-wave velocity. Therefore, it enhances the reliability, speed up geotechnical investigations and also reduces the cost.

1.2 Objectives of study

The objectives of the study are:

- i. To characterize P-wave velocity for two studied area.
- ii. To classify range of P-wave velocity against soil type and stiffness (N-value) of material.

1.3 Scope of study

The research applied seismic refraction tomography to identify subsurface P-wave velocity of residual soil (USM) and sedimentary (Sungai Batu, Kedah) study area. It is attempts to correlate the seismic refraction tomography method with borehole method. Therefore, each survey line is designed crossing an existing

borehole to enhance data interpretation and correlation. However, the study is limited to P-wave velocity (Vp) and standard penetration test (N-value) correlation only. Furthermore, regression between Vp and N-value for both study area were calculated. This topic is only discussed generally and not the main focus of this research.

1.4 Thesis layout

The contents of this thesis are organized as follows;

The first chapter is an introduction of the thesis which provides a general summary of the research framework of the research done which includes problem statement, objectives and scope of study.

Chapter 2 discussed the previous studies regarding soil properties investigation using various types of geophysical methods around the world.

Chapter 3 conferred about the theory of seismic waves and seismic refraction methods, study area, data acquisition and data processing of seismic refraction tomography. The equipment, principle of acquisitions and field procedure are also conversed in this chapter.

Results from seismic refraction tomography and geotechnical techniques were correlated and discussed in chapter 4. Data analysis and regression were also discussed and some parameters were produced from empirical correlations.

Finally, chapter 5 concludes all the objectives of the research and some recommendations and suggestions for future research are also included.

CHAPTER 2

LITERATURE REVIEW

2.0 Introduction

The first seismic survey was carried out in the early 1920s. A great advancement in explosion seismology method is made due to its extensive use as a tool for oil exploration. The method is also employed on a smaller scale mapping of near surface sediment layers. In the last decade, the utilization of geophysics in civil and environmental engineering has become a promising approach.

This chapter present previous study about researchers strive to have knowledge of the correlations between geophysical and geotechnical ground properties to certify reliable interpretation. Various geophysical methods such as 2-D electrical resistivity, seismic and electromagnetic were integrated with geotechnical method such as borehole.

2.1 Theory background

The basic skill of seismic refraction survey is by generating seismic waves at a point on the Earth's surface to travel through subsurface and detected by a number of detectors after being refracted and reflected at geological interfaces between two distinct medium. The detected signals will be displayed on seismograph and recorded for processing and interpretation. The seismic waves are also known as elastic waves.

2.1.1 Elastic wave

Seismic wave behave elastically, hence, called elastic wave and categorized into two types which are body wave and surface wave. Body waves travel through the body of the earth while surface wave is guided along the surface and layers near the surface. All the elastic waves deformed in the form of shear or compressional/dilatational wave (Sharma, 1997).

Body waves are classified into two types; P-wave or primary wave and S-wave or secondary wave. P-wave is also known as longitudinal or compressional wave due to the particle oscillate back and forth during their transport (Figure 2.1). This pressure wave travelled in alternating expansion and contraction of the medium. Sound waves are examples of waves of this category. It has the highest speed among the seismic waves. Therefore, P-waves will arrive first on traces at seismograph. P-waves can travel through solids, liquid and gases (Ismail, 2011).

S-waves are shear or transverse waves. It is called transverse because the particle motion is perpendicular to the direction of the wave travel (Figure 2.2). S-waves also referred as secondary waves because they arrive from an earthquake or seismic source after the P-waves.

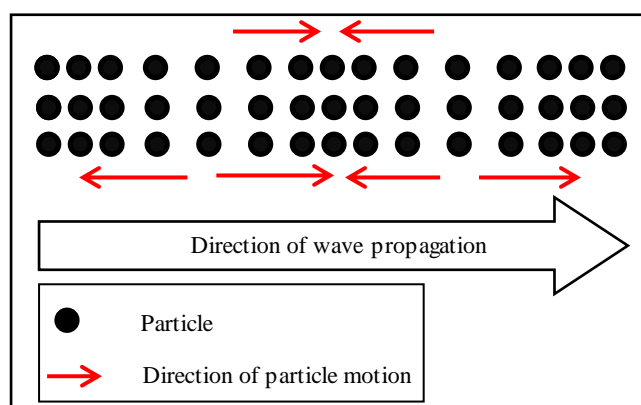


Figure 2.1: Particle move parallel to the direction of wave propagation (Ismail, 2011).

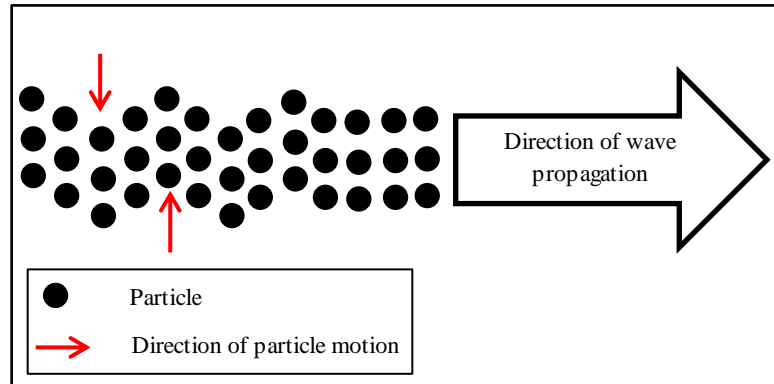


Figure 2.2: Particle move perpendicular to the direction of S-waves propagation (Ismail, 2011).

The velocities of P- and S-waves depend on the elasticity and density of the underground material, thus, can be expressed as (Equation 2.1 and 2.2).

$$V_p = \sqrt{\frac{K + 4\mu/3}{\rho}} \quad (2.1)$$

where;

$$\begin{aligned} K &= \text{Bulk modulus} \\ \mu &= \text{Shear modulus} \\ \rho &= \text{Density} \end{aligned}$$

$$V_s = \sqrt{\frac{\mu}{\rho}} \quad (2.2)$$

where;

$$\begin{aligned} \mu &= \text{Shear modulus} \\ \rho &= \text{Density} \end{aligned}$$

When $\mu = 0$ (as in case for gaseous and liquid medium), P-waves velocity is decreased and the velocity of S-waves become zero (Burger et al., 2006).

Surface wave is the second general type of seismic wave which travel only along the free surface (an interface between the solid and vacuum) of an elastic body.

The wave displacement is lessening as the depth below the surface it travels increases. The velocities of the surface waves are lower than body waves; therefore, they arrive later than P- and S-waves. There are two types of surface waves which are Rayleigh wave and Love wave. The elastic surface wave is a combination of non-uniform longitudinal and shears waves.

Rayleigh wave was named after John William Strutt, Lord Rayleigh, who predicted the existence of this wave mathematically in 1885. The particle motion consists of a combination of compressional and vertical shear (SV) wave vibration, giving rise to an elliptical retrograde motion in the vertical plane along the direction of travel (Figure 2.3). This causes the ground to move side-to-side and up and down. The velocity of Rayleigh wave is about 0.9Vs. During earthquake events, Rayleigh wave causes the strongest shaking effect among other seismic waves.

Love wave was named after Augustus Edward Hough Love, a British mathematician who found this wave mathematically in 1911. It is the fastest surface wave and is confined to the surface. Love wave results from horizontal shear wave (SH) trapped near the surface. Propagation of Love wave causes the ground particles to move side-to-side, perpendicular to the direction of wave (Figure 2.4).

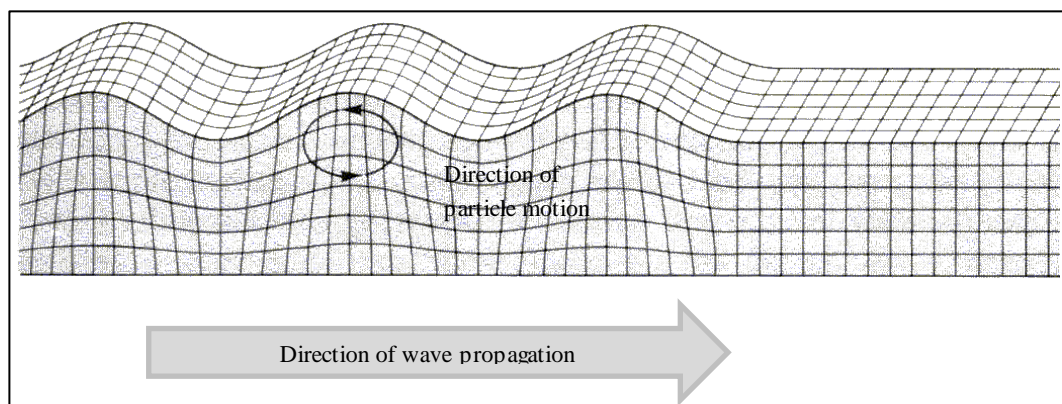


Figure 2.3: Rayleigh wave; particle experience elliptical retrograde motion due to the combination of compressional and vertical shear (SV) waves (Rubin and Hubbard, 2005).

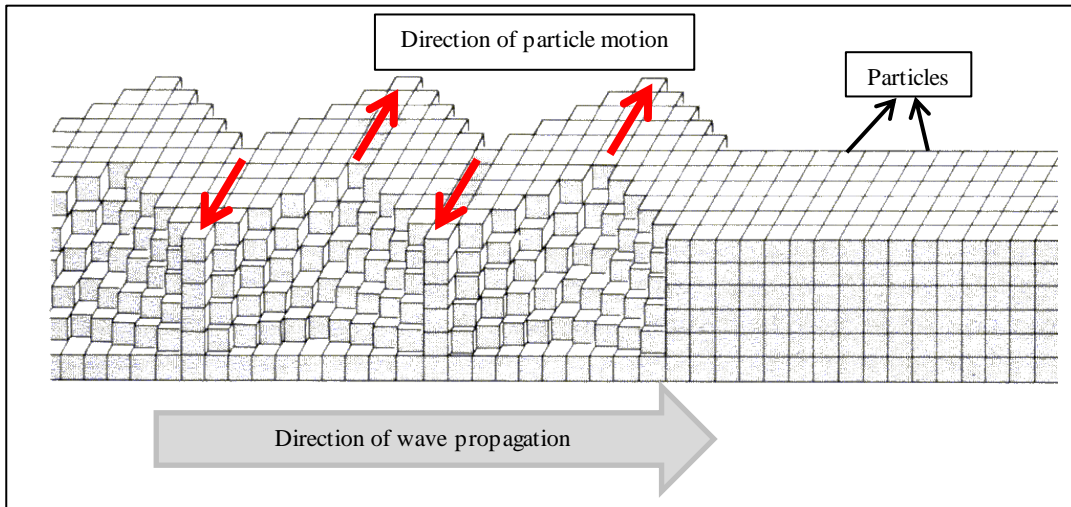


Figure 2.4: Ground particle move side-to-side, perpendicular to the Love wave's propagation (Rubin and Hubbard, 2005).

2.1.2 Wave's propagation principle

Apart from types of seismic waves, it is important to understand the seismic wave's propagation principle. In real situations, wave spreads in three dimensional; spread out like a sphere. The outer shell of the sphere is called wave front and normal to it is called ray path. This principle was developed by Christian Huygens in 1670s and known as Huygens' Principle, which states that every point on the wave front is a source of a new spherical secondary wavelet that travels out. After a time t , the new position of the wave front is the surface of tangent to these wavelets. By applying this principle to the wavefront at t_1 , a new wavefront at t_2 is constructed (Figure 2.5). AB represents the wave front at t_1 while the wave front at t_2 is given by CD with interval time, Δt . The velocity is assumed to be constant throughout the medium and the waves propagate at distance $V\Delta t$ (Burger, 1992).

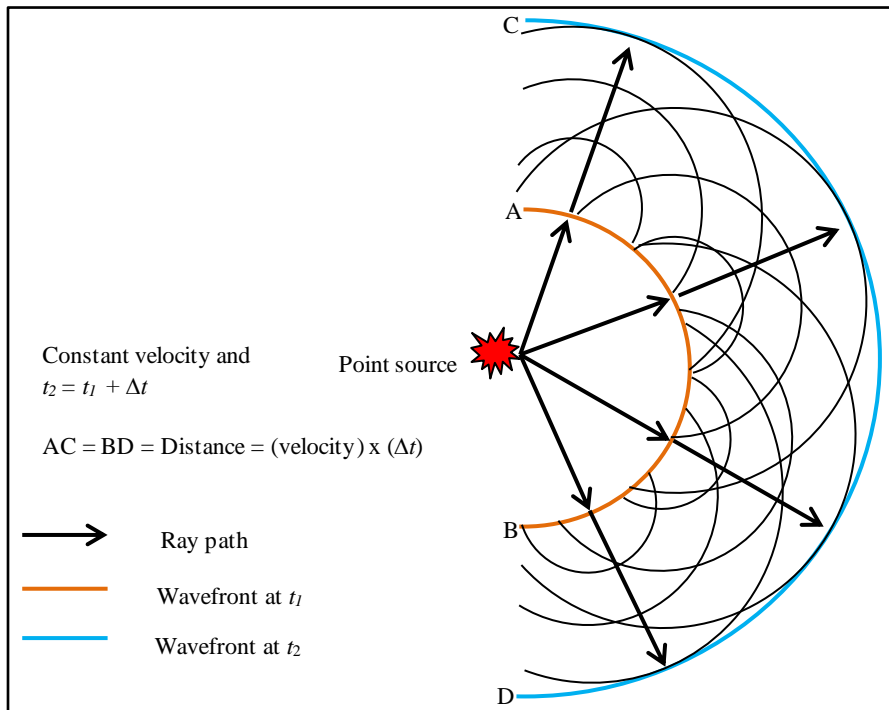


Figure 2.5: Wavefront position at t_2 after an interval of time Δt using Huygens' Principle (Burger, 1992).

By considering only the notion of rays, when a wave front encounter a boundary of different density, some energy is reflected and some is going through the other medium. This situation utilized the fundamental of Snell's Law which relates the angles of incidence and refraction to the seismic velocities of two media (Equation 2.3).

$$\frac{\sin\theta_i}{\sin\theta_r} = \frac{V_1}{V_2} \quad (2.3)$$

where;

θ_i = Incidence angle

θ_r = Refracted angle

V_1 = Velocity of first layer

V_2 = Velocity of second layer

When energy is transmitted from a layer of lower velocity to higher velocity ($V_2 > V_1$), the refraction angle, θ_r is greater than the incidence angle, θ_i . As the

incidence angle, θ_i , increases, there is a unique case when refracted angle, $\theta_r = 90^\circ$ and $\sin \theta_r = 1$. In this case the angle is known as critical angle of incidence, θ_{ic} . For incidence angle greater than θ_{ic} , the energy is totally reflected into the upper layer (Figure 2.6) (Bengt, 1984).

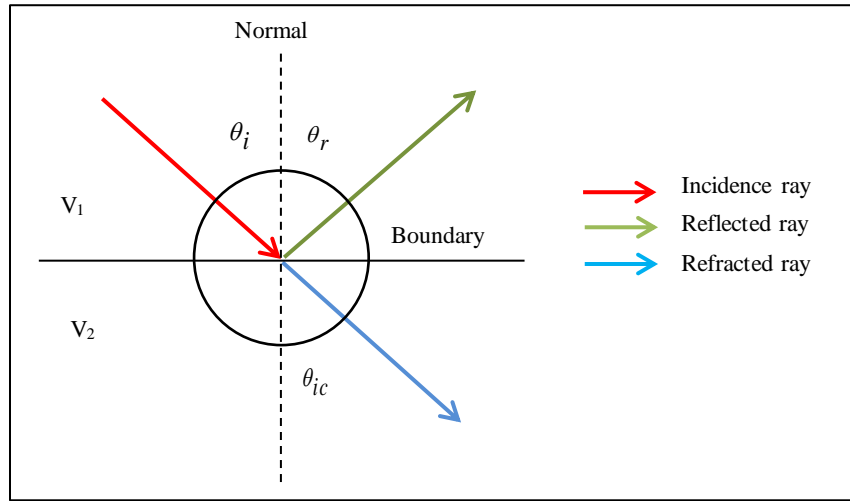


Figure 2.6: Schematic diagram of Snell's Law (Bengt, 1984).

2.1.3 Homogeneous subsurface

When seismic waves propagate in a homogeneous subsurface, it travel with constant velocity and the equally spaced geophones record the ground displacement. With the information of geophone spacing, distance from shot point to the first geophone (shot offset) and arrival time of waves to each geophone, a time-distance graph can be plotted, which produce a straight line (Figure 2.7) (Burger et al., 2006).

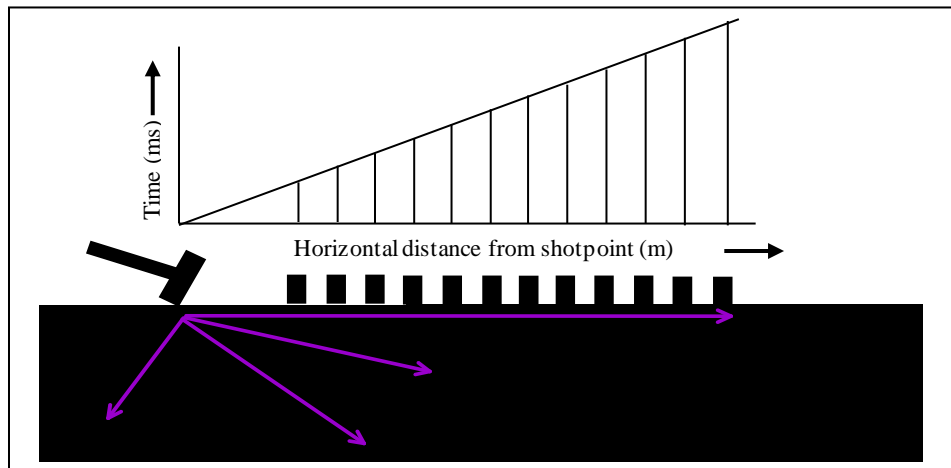


Figure 2.7: Ray paths in homogeneous subsurface (Burger et al., 2006).

From the time-distance graph, arrival time, t of direct wave is given by Equation 2.4.

$$t = \frac{x}{V_1} \quad (2.4)$$

where;

$$\begin{aligned} x &= \text{Distance from shotpoint to receiver (m)} \\ V_1 &= \text{Velocity of first layer (m/s)} \end{aligned}$$

By taking the first derivative of the equation with respect to x , the velocity is obtained (Equation 2.5 and 2.6)

$$\frac{dt}{dx} = \frac{1}{V_1} \quad (2.5)$$

Therefore;

$$V_1 = \frac{1}{\text{slope}} \quad (2.6)$$

$$\text{where;} \quad \frac{dt}{dx} = \text{slope}$$

2.1.4 Single subsurface interface (2 layer case)

In real situations, subsurface is usually not homogeneous. Therefore, several interfaces are present. These interfaces cause reflections, refractions and wave conversions. This study is limited to only refraction case. A compressional wave generated at energy source, S travelling at velocity V_1 strikes the interfaces between materials with different velocity, V_2 . The ray that strikes the interface at critical angle, θ_{ic} is refracted parallel to the interface and travel with velocity V_2 and returned to the surface at velocity, V_1 through QG (Figure 2.8). Figure 2.9 shows the wave velocity of the first layer, V_1 and second layer, V_2 and thickness of layer 1, h_1 is obtained from the travel time curve (Burger, 1992).

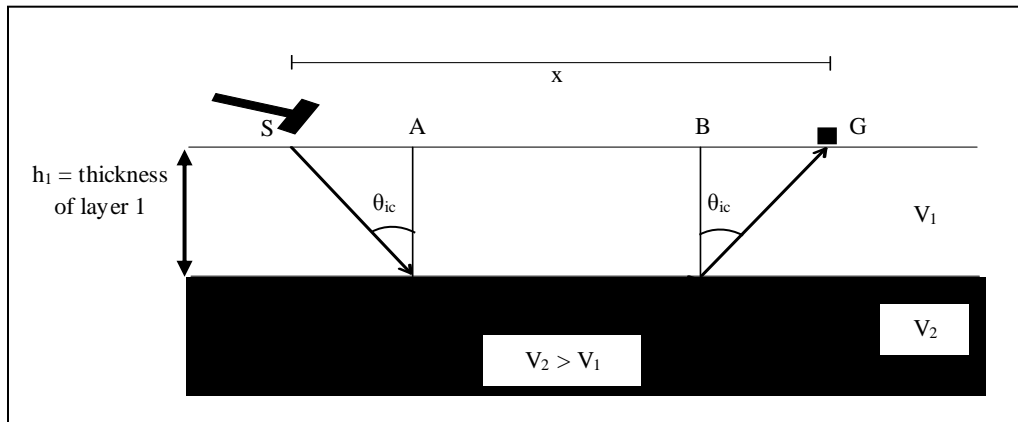


Figure 2.8: Refracted ray path for a single subsurface interface (Burger et al., 2006).

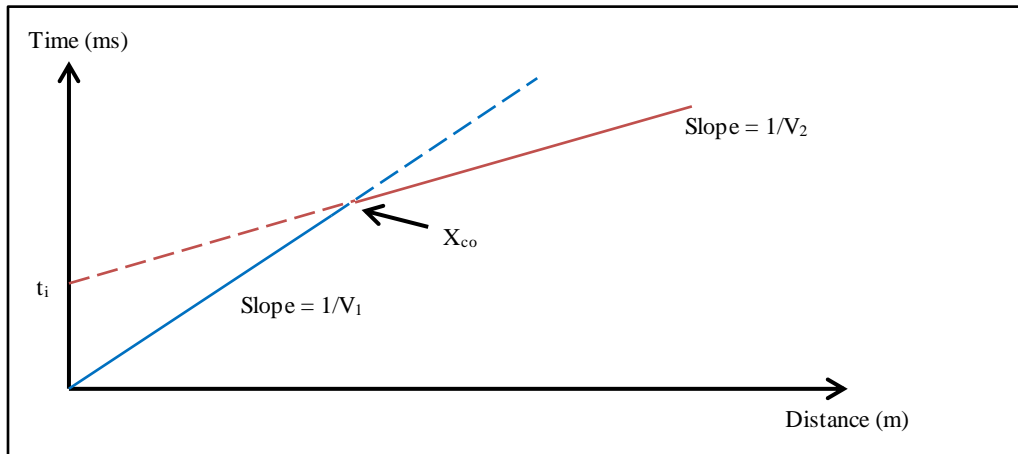


Figure 2.9: Travel time curve for a single subsurface interface (Burger et al., 2006).

The total travel time is defined in Equation 2.7 - 2.13

$$\text{time} = \frac{SP}{V_1} + \frac{PQ}{V_1} + \frac{QG}{V_1} \quad (2.7)$$

$$\cos\theta_{ic} = \frac{h_1}{SP} \quad (2.8)$$

$$SP = QG = \frac{h_1}{\cos\theta_{ic}} \quad (2.9)$$

$$SA = BG = h_1 \tan\theta_{ic} \quad (2.10)$$

$$PQ = x - 2h_1 \tan\theta_{ic} \quad (2.11)$$

Therefore,

$$\text{time} = \frac{h_1}{V_1 \cos\theta_{ic}} + \frac{x - 2h_1 \tan\theta_{ic}}{V_2} + \frac{h_1}{V_1 \cos\theta_{ic}} \quad (2.12)$$

Equation 3.12 is the simplified to Equation 3.13

$$\text{time} = \frac{x}{V_2} + \frac{2h_1 \sqrt{(V_2)^2 - (V_1)^2}}{V_1 V_2} \quad (2.13)$$

where;

- SP = Distance between points S and P
- PQ = Distance between points P and Q
- QG = Distance between points Q and G
- V_1 = Velocity of first layer (m/s)
- V_2 = Velocity of second layer (m/s)
- h_1 = Thickness of first layer (m)
- x = Distance between points S and G (m)
- θ_{ic} = Incidence critical angle

The thickness of the material above the interface is determined using two methods; intercept time, t_i and crossover distance, x_{co} .

The intercept time method assumes no refractions arrive at the energy source, $x = 0$, therefore, $t = t_i$. Equation 2.13 reduces to Equation 2.14 and thickness of first layer is given by Equation 2.15.

$$\text{time} = t_i = \frac{2h_1 \sqrt{(V_2)^2 - (V_1)^2}}{V_1 V_2} \quad (2.14)$$

Therefore,

$$h_1 = \frac{t_i V_1 V_2}{2 \sqrt{(V_2)^2 - (V_1)^2}} \quad (2.15)$$

For crossover distance method, an intersection point between direct wave and refracted wave is known as crossover distance, X_{co} . At this point, the times for direct and refracted waves are equal. Depth to the interface, h_1 is calculated using Equation 2.16.

$$h_1 = \frac{X_{co} \sqrt{V_2 - V_1}}{2 \sqrt{V_2 + V_1}} \quad (2.16)$$

where;

$$\begin{aligned} V_1 &= \text{Velocity of first layer (m/s)} \\ V_2 &= \text{Velocity of second layer (m/s)} \\ X_{co} &= \text{Crossover distance (m)} \end{aligned}$$

2.1.5 Factors effecting velocity

Seismic velocity is a function of density and elastic properties of wave propagation medium. The actual seismic velocities in rock materials depend on a lot of factors including mineral content, grain size, temperature, cementation, fabric, porosity, weathering, confining pressure and fluid content. Seismic velocity of the major rock forming minerals is higher than those of the fresh rocks which they form. Post formation processes such as weathering, fracturing and structural deformation decrease the velocity although thermal recrystallizations increase rock strength and velocity. Due to these factors, seismic velocities in shallow Earth materials are highly variable.

Generally, a hard crystalline rock is the greatest seismic velocity, while the unconsolidated materials, seismic velocities are least. Some of sedimentary rock such as limestone and dolomite may have seismic velocity greater than some fresh metamorphic and igneous rock due to the effect of compaction and lithification. There are no distinctive values of velocities for rocks or sediments, however there are five basic rules that influence the velocity of the material. Firstly, the unsaturated sediments have lower values than saturated sediment. Secondly, the unconsolidated sediment has lower values than consolidated sediments followed by third rule which velocity is similar in saturated and unconsolidated sediments. Rule number four is weathered rocks has lower value than a similar rock that are unweathered and last but not least is the fractured rocks have lower values than similar rocks that are unfractured (Laric and Robert, 1987). Table 2.1 shows the velocity range of common materials.

Table 2.1: P-wave velocity of common materials (Press, 1966).

Unconsolidated materials (m/s)		Consolidated materials (m/s)		Other (m/s)	
Weathered layer	300-900	Granite	5000-6000	Water	1400-1600
Soil	250-600	Basalt	5400-6400	Air	331.5
Alluvium	500-2000	Metamorphic rocks	3500-7000		
Clay	1100-2500	Sandstone and shale	2000-4500		
Sand		Limestone	2000-6000		
Unsaturated	200-1100				
Saturated	800-2200				
Sand and gravel					
Unsaturated	400-500				
Saturated	500-1500				
Glacial till					
Unsaturated	400-1000				
Saturated	1700				
Compacted	1200-2100				

2.2 Geotechnical investigation

Geotechnical technique is widely utilized in subsurface explorations around the world. It is used to obtain information about subsurface soil conditions. The method normally applied at a proposed construction site. This geotechnical method is

divided into several techniques which are test pits, trenching, boring and in-situ test. This study utilized boring and in-situ test technique known as rotary wash boring (RWB) and standard penetration test (SPT).

2.2.1 Rotary wash boring (RWB)

In geophysics study, borehole is used to correlate sedimentary, stratigraphy and structural analysis in order to validate the result obtained. RWB is a combination of two methods; wash boring and rotary drilling. Therefore, it consists of two stages; boring and coring. Boring is process of drilling in soil while coring is in rock. Samples were taken during both stages. The coring sample is then tested for Core Recovery Ratio (CRR) and Rock Quality Designation (RQD). CRR is the ratio length of good quality cores over the drilling length expressed to the nearest 5% while RQD is ratio of the total length of good quality cores each exceeding 100 mm in length over the drilling. The six different types of boring and drilling that are widely used are wash boring, auger boring, displacement boring, rotary drilling, percussion drilling and continuous sampling (Wazoh and Mallo, 2014).

2.2.2 Standard Penetration Test (SPT)

Standard penetration test (SPT) is an in-situ test designed to provide information on the geotechnical engineering properties of soil and carried out during drilling process. A sample tube of 0.65 m length is driven into the ground at the bottom of a borehole by blows from a hammer with a weight of 63.5 kg falling through a distance of 7.6 m. The sample tube is driven into the ground up to 0.45 m depth. The number of blows (hammer) needed for the tube to penetrate each 0.15 m (6 in) is recorded. The number of blows required to drive the tube is termed as

"standard penetration resistance" or the "N-value". The tube is divided into 3 increments of 0.15 m each (Figure 2.10).

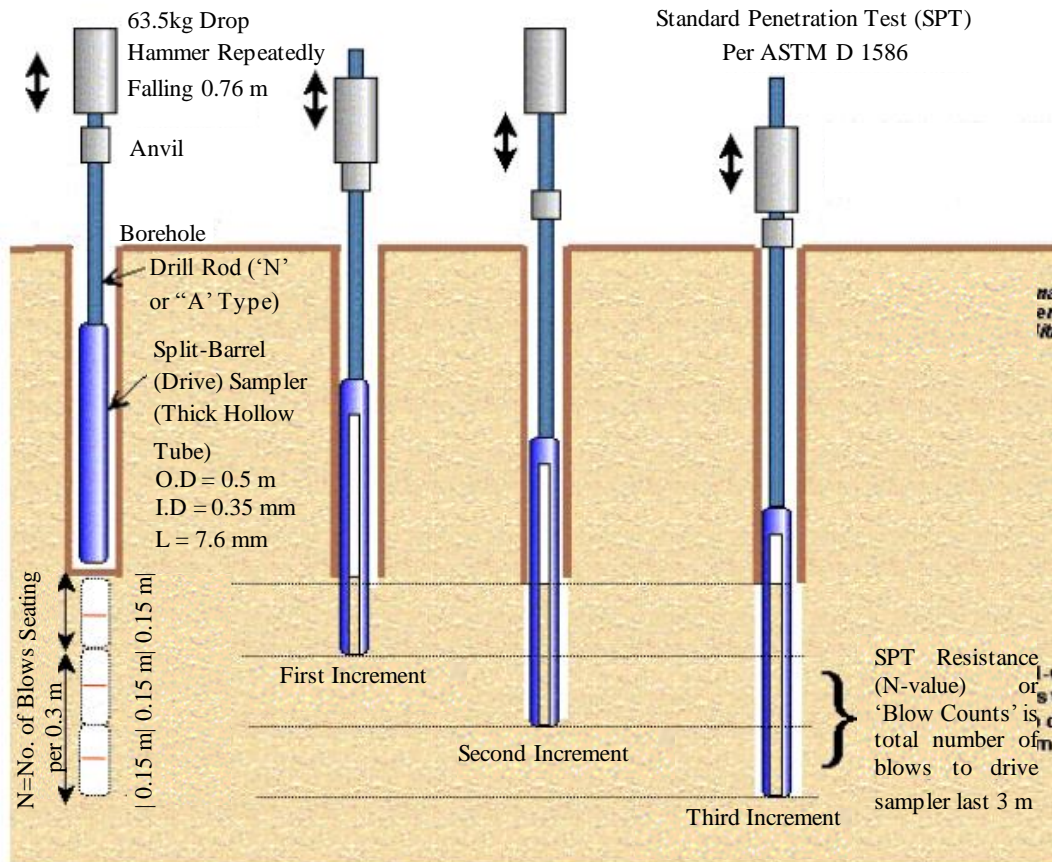


Figure 2.10: Standard penetration test method (Wazoh and Mallo, 2014).

The number of blows for the first increment is not counted and it is known as seating drive. While the total number of blows for the second and third increment is counted and called "standard penetration resistance" or the "N-value". The SPT is done repeatedly at every 0.15 m depth until reaching bedrock (ASTM, 2011).

2.3 Previous study

Azwin et al. (2015) performed geophysical and geotechnical methods to verify the type of the crater and characteristics accordingly at Bukit Bunuh, Malaysia. This paper presents the combined analysis of 2-D electrical resistivity,

seismic refraction, geotechnical N-value (Standard Penetration Test), moisture content and RQD within the study area. Bulk P-wave seismic velocity and resistivity were digitized from seismic and 2-D resistivity sections at specific distance and depth for corresponding boreholes and samples. Standard table of bulk P-wave seismic velocity and resistivity against N-value, moisture content and RQD are produced according to geological classifications of impact crater; inside crater, rim/slumped terrace and outside crater (Table 2.2-2.4).

Table 2.2: Impacted soil and rock standard table for inside crater of Bukit Bunuh impact crater.

Geological classification	Resistivity, ρ (m)	P-wave velocity, V_p (m/s)	N-value	Moisture content, MC	RQD (%)
Post-impact sediment fill deposit -clay and silt -sand and gravel	100-700 300-5000	375-800 800-2100	0-24 10-23	18-59 12-27	
Rocks -Slightly weathered granite Class C Class D	1050-2500 900-5800	1500-2500 1200-2700			70-100 27-50

Table 2.3: Impacted soil and rock standard table on rim/slumped terrace of Bukit Bunuh impact crater.

Geological classification	Resistivity, ρ (m)	P-wave velocity, V_p (m/s)	N-value	Moisture content, MC	RQD (%)
Post-impact sediment fill deposit -silt -sand and gravel	70-500 540-3150	400-800 900-3600	2-39 10-50	17-30 14-26	
Rocks -Highly weathered granite -Moderately weathered granite -Slightly weathered granite Class D	290-530 250-620 330-500	3200 1800-3300 1700-3100			0 0 17-86

Table 2.4: Impacted soil and rock standard table for outside crater of Bukit Bunuh impact crater.

Geological classification	Resistivity, ρ (m)	P-wave velocity, V_p (m/s)	N-value	Moisture content, MC	RQD (%)
Post-impact sediment fill deposit					
-silt	55-60	650-700	16-19	18-22	
-sand and gravel	100-420	740-1100	17-50	17-19	
Rocks					
-Slightly weathered granite	1545-1600	2100-2200			0
Class C	870-1150	1500-1900			67-77
Class D	650-700	1260-1300			91.6

Awang and Mohamad (2016) develop correlation between P-wave velocity from seismic refraction method against N-value from existing borehole data. The study area was located at Bandar Country Homes, Rawang, Selangor which underlain by Terolak Formation. Three seismic lines were conducted across six existing boreholes with the aim to characterize the subsurface of the study area. This study summarizes the seismic result correlated to borehole record as shown in Table 2.5.

Table 2.5: Correlation of P-wave velocity and N-value.

Layer	Velocity (m/s)	Depth (m)	Description
1	<500	<13 (from existing ground level)	Soil (gravelly sandy SILT)
2	2200-3000	13-18	Sand (water saturated, loose)
3	>3000	>18 (from existing ground level)	Sandstone (bedrock)

Taib and Hasan (2002) presented a case study at Shah Alam and Sungai Buloh, Selangor which utilizes geophysical method and geotechnical method (borehole). The seismic refraction velocities were correlated with SPT N-values and mackintosh probe (M-value). The research found that M-value of <400 is comparable directly with velocity layer of <500 m/s, while N-value of <30 is correspond to the second layer velocity of 500-1650 m/s. These correlation results give a more meaningful interpretation for future study.

Ulugergerli and Uyanik (2007) conducted a research to study the correlation between N-value, seismic (P and S-wave) velocities and relative density. The research is focused on the variations of seismic velocities with relative density and N-value with seismic velocities. Instead of using the conventional approach to fit the data with best single curve, the authors define empirical relationships as upper and lower boundaries considering the scattered nature of the data; so that the large range can represent a whole span of observation of the site. It was discovered that the upper limits generated model of N-value and density as natural logarithmic functions (Table 2.6). The result was further presented as both narrow and wide ranges of limits. For the wide ranges, it was recommended that direct field measurements must be employed to ascertain accurate measurement of any geotechnical parameters.

Table 2.6: The relation between V_p , V_s , N-value and density (Ulugergerli and Uyanik, 2007).

	P-wave velocity, V_p (m/s)	S-wave velocity, V_s (m/s)
N-value	$N_U = 119.55 \ln(V_p) - 644.36$	$N_U = 113.41 \ln(V_s) - 469.32$
	$N_L = 9.014 e^{-0.0004V_p}$	$N_L = 7.1737 e^{-0.0013V_s}$
Density (gr/cm ³)	$\text{Density}_U = 0.0723 \ln(V_p) + 1.4741$	$\text{Density}_U = 0.1055 \ln(V_p) + 1.3871$
	$\text{Density}_L = 1.7114 e^{-0.00003V_p}$	$\text{Density}_L = 1.6007 e^{-0.0002V_p}$

Bery and Saad (2013) correlating P-wave velocities with N-value and other engineering physical parameters such as rock quality, friction angle, relative density, velocity index, penetration strength and density. Empirical correlations of N-values and rock quality designation (RQD) with P-wave velocities were found as $V_p=23.605(N)-160.43$ and $V_p=21.951(RQD)+0.1368$ with regression is 0.9315 (93.15%) and 0.8377 (83.77) respectively (Figure 2.11). This study contributes in estimating and predicting properties of subsurface material (soils and rocks) to reduce the cost of investigation and increase the understanding of the Earth's subsurface characterizations physical parameters.

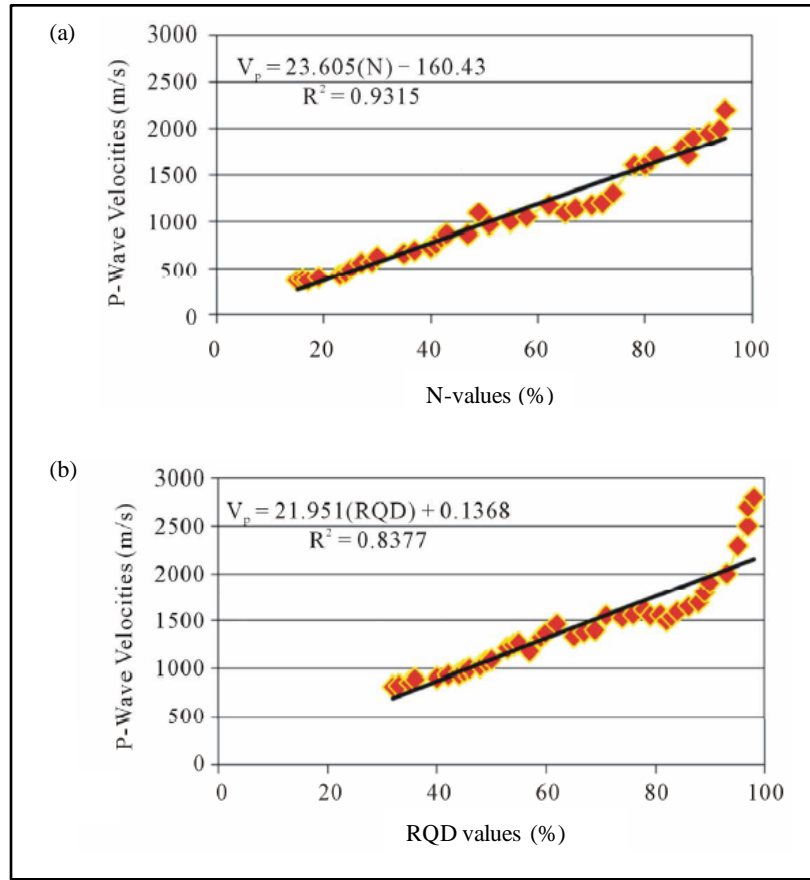


Figure 2.11: Empirical correlation of (a) P-wave velocities with N-values and (b) P-wave velocities with RQD values for both studied areas (Bery and Saad, 2013).

A new relationship between SPT-N and shear velocity (Vs) was proposed by Fauzi et al. (2014). The study was conducted at 22 building project and 35 borings in Jakarta. This study utilized seismic downhole method at each borehole and results a total of 234 pairs of SPT-N and Vs values were obtained. The seismic downhole were performed at 1.0 m interval. SPT was conducted at interval of 1.5-2 m and it is follow the ASTM D 1586-84 standards. The equation is computed by statistical regression, $Vs=105.03N^{0.286}$ with regression, $R^2 = 0.675$. The results from the comparisons between new and previously proposed equations show that some correlations fit the data points reasonably well. However, specific geotechnical condition of the site, the quality of processed data and the procedure used in undertaking the SPTs and seismic survey causes some deviations.

Anbazhagan et al. (2012) conducted multichannel analysis of surface wave (MASW) to measure shear waves (V_s) velocities. The method was applied using 24 channels Geode seismograph with 24 vertical geophones of 4.5 Hz capacity. The studies were carried out at a number of site responses. The main purpose of this study is to produce a new correlation between shear modulus and N-values. The previously available correlations were studied and compared with the new correlation. The result shows that the correlation; $G_{max} = 16.4N^{0.65}$ has higher regression coefficient of $R^2 = 0.85$.

Bang and Kim (2007) proposed a SPT up-hole method which using the impact energy of the split spoon sampler in SPT test as the seismic energy source. Many field test such as harmonic wavelet analysis of waves (HWAW), spectral analysis of surface wave (SASW), multi-channel analysis of surface wave (MASW), suspension PS logging, down-hole and cross-hole are widely used for an evaluation of the V_s profile. The study was conducted at four different sites in order to verify the proposed SPT up-hole method. Data were compared with SASW and down-hole methods as well as the N-values. The SASW was performed at the same line with the SPT up-hole method and the results show that the V_s profiles matches well each other.

Hasancebi and Ulusay (2007) made an attempt to create a new relationship between N-value and V_s to estimate V_s . The study was based on geophysical (seismic refraction) and geotechnical data from Yenisehir settlement, located in Marmara region of Turkey. The variations of shear wave velocity were measured and a series of empirical equations were developed and compared with the previously suggested empirical equations. The study conclude that new regression equations